Inorganic Chemistry
Article

Inorg. Chem. **2009**, *48*, 5303–5312 **5303**
DOI: 10.1021/ic900342j

Volatility, High Thermal Stability, and Low Melting Points in Heavier Alkaline Earth Metal Complexes Containing Tris(pyrazolyl)borate Ligands

Mark J. Saly, Mary Jane Heeg, and Charles H. Winter*

Department of Chemistry, Wayne State University, Detroit, Michigan 48202

Received February 23, 2009

Treatment of MI_2 (M = Ca, Sr) or $\text{BaI}_2(\text{THF})_3$ with 2 equiv of potassium tris(3,5-diethylpyrazolyl)borate (KTp^{Et2}) or potassium tris(3,5-di-*n*-propylpyrazolyl)borate (KTp^{nPr2}) in hexane at ambient temperature afforded $\text{CaTp}_2^{\text{Et2}}$ (64%), $\text{SrTp}_2^{\text{Et2}}$ (64%), $\text{BaTp}_2^{\text{Et2}}$ (67%), $\text{CaTp}_2^{\text{nPr2}}$ (51%), $\text{SrTp}_2^{\text{nPr2}}$ (75%), and $\text{BaTp}_2^{\text{nPr2}}$ (39%). Crystal structure determinations of $\text{CaTp}_2^{\text{Et2}}$, $\text{SrTp}_2^{\text{Et2}}$, and $\text{BaTp}_2^{\text{Et2}}$ revealed monomeric structures. X-ray structural determinations for strontium tris(pyrazolyl)borate (SrTp_2) and barium tris(pyrazolyl)borate ($[\text{BaTp}_2]_2$) show that SrTp_2 exists as a monomer and $[\text{BaTp}_2]_2$ exists as a dimer containing two bridging Tp ligands. The thermogravimetric analysis traces, preparative sublimations, and melting point/decomposition determinations demonstrate generally very high thermal stabilities and reasonable volatilities. SrTp_2 has the highest volatility with a sublimation temperature of 200 °C/0.05 Torr. $[\text{BaTp}_2]_2$ is the least thermally stable with a decomposition temperature of 330 °C and a percent residue of 46.5% at 450 °C in the thermogravimetric analysis trace. $\text{SrTp}_2^{\text{Et2}}$, $\text{BaTp}_2^{\text{Et2}}$, $\text{CaTp}_2^{\text{nPr2}}$, $\text{SrTp}_2^{\text{nPr2}}$, and $\text{BaTp}_2^{\text{nPr2}}$ vaporize as liquids between 210 and 240 °C at 0.05 Torr. $\text{BaTp}_2^{\text{Et2}}$ and $\text{BaTp}_2^{\text{nPr2}}$ decompose at about 375 °C, whereas $\text{MTp}_2^{\text{Et2}}$ and $\text{MTp}_2^{\text{nPr2}}$ (M = Ca, Sr) are stable to >400 °C. Several of these new complexes represent promising precursors for chemical vapor deposition and atomic layer deposition film growth techniques.

Introduction

The heavier group 2 elements are constituents in many important solid state materials,[1] including high k dielectrics for dynamic random access memories (SrTiO_3, $(\text{Sr,Ba})\text{TiO}_3$),[2,3] ferroelectric phases for computer memory devices (BaTiO_3, $\text{SrBi}_2\text{Ta}_2\text{O}_9$),[4,5] high-$T_c$ superconductors ($\text{YBa}_2\text{Cu}_3\text{O}_{7-x}$, $\text{La}_{1-x}\text{Ca}_x\text{MnO}_3$),[6] electroluminescent devices (SrS:Ce, BaS:Ce),[7] and nonlinear optical crystals (β-BaB_2O_4).[8] For many applications, these materials must be grown as thin films. Chemical vapor deposition[9] (CVD) and atomic layer deposition[10] (ALD) are two powerful film growth methods. Both techniques require precursors that volatilize at moderate temperatures without decomposition. In addition, ALD requires precursors that are thermally stable at the substrate temperature to avoid loss of the self-limited growth mechanism.[10] Unfortunately, currently available CVD and ALD precursors for calcium, strontium, and barium are

---

*To whom correspondence should be addressed. E-mail: chw@chem.wayne.edu.

(1) For recent reviews, see: (a) Wojtczak, W. A.; Fleig, P. F.; Hampden-Smith, M. J. *Adv. Organomet. Chem.* **1996**, *40*, 215–340. (b) Guglielmo, G. G.; Malandrino, G.; Ignazio, F. L. *Coord. Chem. Rev.* **2007**, *251*, 1931–1948. (c) Wessels, B. W. *Annu. Rev. Mater. Sci.* **1995**, *25*, 525–546. (d) Matthews, J. S.; Rees, W. S.Jr. *Adv. Inorg. Chem.* **2000**, *50*, 173–192.

(2) Selected examples: (a) Gilbert, S. R.; Wessels, B. W.; Studebaker, D. B.; Marks, T. J. *Appl. Phys. Lett.* **1995**, *66*, 3298–3300. (b) Sone, S.; Yabuta, H.; Kato, Y.; Iizuka, T.; Yamamichi, S.; Yamaguchi, H.; Lesaicherre, P.; Nishimoto, S.; Yoshida, M. *Jpn. J. Appl. Phys.* **1996**, *35*, 5089–5093. (c) Kang, C. S.; Hwang, C. S.; Cho, H. J.; Lee, B. T.; Park, S. O.; Kim, J. W.; Horii, H.; Lee, S. I.; Koh, Y. B.; Lee, M. Y. *Jpn. J. Appl. Phys.* **1996**, *35*, 4890–4895.

(3) Hwang, C. S. *Mater. Sci. Eng., B* **1998**, *56*, 178–190.

(4) Selected examples: (a) Wills, L. A.; Wessels, B. W.; Richeson, D. S.; Marks, T. J. *Appl. Phys. Lett.* **1992**, *60*, 41–43. (b) Chandler, C. D.; Roger, C.; Hampden-Smith, M. J. *Chem. Rev.* **1993**, *93*, 1205–1241. (c) Towner, D. J.; Marks, T. J.; Wessels, B. W. *J. Cryst. Growth* **2003**, *255*, 107–113. (d) Zhang, J.; Beetz, C. P.Jr; Krupanidhi, S. B. *Appl. Phys. Lett.* **1994**, *65*, 2410–2412. (e) Dhote, A. M.; Meier, A. L.; Towner, D. J.; Wessels, B. W.; Ni, J.; Marks, T. J. *J. Vac. Sci. Technol. B* **2005**, *23*, 1674–1678.

(5) (a) Amanuma, K.; Hase, T.; Miyasaka, Y. *Appl. Phys. Lett.* **1995**, *9*, 221–223. (b) Araujo, C. A.; Cuchiaro, J. D.; McMillan, L. D.; Scott, M. C.; Scott, J. F. *Nature (London)* **1995**, *374*, 627–629. (c) Melgarejo, R. E.; Tomar, M. S.; Dobal, P. S.; Katiyar, R. S. *J. Mater. Res.* **2000**, *15*, 1661–1664.

(6) (a) Geballe, T. H.; Hulm, J. K. *Science* **1988**, *239*, 367–375. (b) Horowitz, H. S; McLain, S. J.; Seight, A. W.; Druliner, J. D.; Gai, P. L.; VanKavelaar, M. J.; Wagner, J. L.; Biggs, B. D.; Poon, S. J. *Science* **1989**, *243*, 66–69. (c) Hubert-Pfalzgraf, L. G.; Guillon, H. *Appl. Organomet. Chem.* **1998**, *12*, 221–236. (d) Nilsen, O.; Rauwel, E.; Fjellvag, H.; Kjekshus, A. *J. Mater. Chem.* **2007**, *17*, 1466–1475.

(7) (a) Tammenmaa, M.; Anstson, H.; Asplund, M.; Hiltunen, L.; Leskelä, M.; Niinistö, L. *J. Cryst. Growth* **1987**, *84*, 151–154. (b) Saanila, V.; Ihanus, J.; Ritala, M.; Leskelä, M. *Chem. Vap. Deposition* **1998**, *4*, 227–233. (c) Ihanus, J.; Hänninen, T.; Hatanpää, T.; Aaltonen, T.; Mutikainen, I.; Sajavaara, T.; Keinonen, J.; Ritala, M.; Leskelä, M. *Chem. Mater.* **2002**, *14*, 1937–1944. (d) Ihanus, J.; Hänninen, T.; Hatanpää, T.; Ritala, M.; Leskelä, M. *J. Electrochem. Soc.* **2004**, *151*, H221–H225.

(8) (a) Lin, J. T. *Opt. Quantum Electron.* **1990**, *22*, S283–S313. (b) Studebaker, D. B.; Stauf, G. T.; Baum, T. H.; Marks, T. J.; Zhou, H.; Wong, G. K. *Appl. Phys. Lett.* **1997**, *70*, 565–568. (c) Malandrino, G.; Nigro, R. L.; Fragalà, I. L. *Chem. Vap. Deposition* **2007**, *13*, 651–655. (d) Wersand-Quell, S.; Orsal, G.; Thévenin, P.; Bath, A. *Thin Solid Films* **2007**, *515*, 6507–6511.

(9) (a) Pierson, H. O. *Handbook of Chemical Vapor Depostion (CVD)*; Noyes Publications/William Andrew Publishing: Norwich, NY, 1999.(b) Hitchman, M. L.; Jenson, K. F. *Chemical Vapor Deposition: Principles and Applications*; Academic Press: London, 1993.

(10) For recent reviews, see: (a) Leskelä, M.; Ritala, M. *Angew. Chem., Int. Ed.* **2003**, *42*, 5548–5554. (b) Niinistö, L.; Päiväsaari, J.; Niinistö, J.; Putkonen, M.; Nieminen, M. *Phys. Status Solidi. A* **2004**, *201*, 1443–1452. (c) Putkonen, M.; Niinistö, L. *Top. Organomet. Chem.* **2005**, *9*, 125–145.

plagued by low volatility, generally poor thermal stability, and inappropriate reactivity. These issues can be attributed to the small charge-to-size ratios and low Lewis acidities of the metal ions.[1] Many different ligands have been employed to create volatile CVD precursors of the heavier group 2 elements because of the less stringent thermal stability requirement in this growth technique. These include complexes containing β-diketonate,[1b,11,12] β-ketoiminate,[13] β-diketiminate,[14] alkoxide,[15] pyrazolate,[16] and cyclopentadienyl[17] ligands. State of the art CVD precursors are exemplified by fluorinated β-diketonate complexes containing neutral polydentate ether ligands[12] and β-ketoiminato complexes with appended polyether substituents.[13] The former class sublimes well at reasonable temperatures (120−160 °C), but the presence of fluorine is a liability, since this element is easily incorporated into the thin films and can lead to changes in materials properties. The latter class does not contain fluorine but decomposes in the solid state concurrently with sublimation.[13] There have been few reports of the growth of strontium- and barium-containing materials by ALD because of a critical lack of precursors that combine acceptable volatility, thermal stability, and high reactivity toward an oxygen-based precursor. The β-diketonate precursors "Sr(thd)$_2$" and "Ba(thd)$_2$" (thd = 2,2,6,6-tetramethylheptane-3,6-dionato) have been employed along with hydrogen sulfide for the growth of SrS, BaS, and BaS:Ce thin films by ALD.[7a,7b,18] These group 2 precursors have very low vapor pressures because of their oligomeric structures.[19] In addition, "Sr(thd)$_2$" and "Ba(thd)$_2$" have low reactivity, and cannot serve in ALD processes employing water as the oxygen precursor under normal thermal growth conditions. However, $SrTiO_3$ films were grown by ALD with "Sr(thd)$_2$", Ti(OiPr)$_4$, and either remote plasma-activated water vapor or remote oxygen plasma.[20] Cyclopentadienyl precursors of strontium and barium are much more reactive toward water and are the only other class of precursors for which oxide ALD growth studies have been reported.[21] A range of alkyl-substituted cyclopentadienyl ligands has been used to create volatile strontium and barium precursors, but Sr(C_5H_2iPr$_3$)$_2$ and Ba(C_5H_2tBu$_3$)$_2$ or tetrahydrofuran (THF) adducts thereof provided the best performance in the ALD growth of $SrTiO_3$, $BaTiO_3$, SrS, and BaS thin films.[7c,7d,21] Ba(C_5H_2tBu$_3$)$_2$ may be thermally stable at up to 350 °C as a solid and was employed for the ALD growth of $BaTiO_3$ films at substrate temperatures of up to 325 °C but is too reactive for use in CVD.[21d] However, Sr(C_5H_2iPr$_3$)$_2$ showed evidence for thermal decomposition at the temperatures required for crystalline $SrTiO_3$ ALD film growth.[21d,21f]

We have recently reported the ALD growth of Ta_2O_5 films from Ta(NtBu)(tBu$_2$pz)$_3$ (tBu$_2$pz = 3,5-di-*tert*-butylpyrazolate) and ozone.[22] Significantly, an ALD window was observed between 300 and 450 °C, implying that Ta(NtBu)(tBu$_2$pz)$_3$ is stable in this temperature range. The only possible source of this exceptional thermal stability was the tBu$_2$pz ligand. We sought to employ the favorable attributes of pyrazolate ligands to prepare thermally stable group 2 complexes that might be useful in ALD film growth. The complexes Ca$_3$(tBu$_2$pz)$_6$, Sr$_4$(tBu$_2$pz)$_8$, and Ba$_6$(tBu$_2$pz)$_{12}$ have been reported but have very low vapor pressures because of their oligomeric structures.[16e] Monomeric group 2 bis(pyrazolate) complexes containing neutral donor ligands decompose extensively upon heating, and do not possess sufficient thermal stability for use in ALD because of neutral ligand loss.[16a−16d] Accordingly, we turned our attention to tris(pyrazolyl)borate-based ligand systems. Tris(pyrazolyl)borate ligands generally coordinate to metal ions in a tridentate fashion through the 2-nitrogen atoms, and additional stability can be obtained through introduction of alkyl substituents in the 3- and 5-positions of the pyrazolyl rings.[23,24] Previously, it was shown that calcium, strontium, and barium complexes containing tris(3,5-dimethylpyrazolyl)borate (Tp^{Me2}) ligands form volatile

---

(11) Selected examples: (a) Purdy, A. P.; Berry, A. D.; Holm, R. T.; Fatemi, M.; Gaskill, D. K. *Inorg. Chem.* **1989**, *28*, 2799–2803. (b) Norman, J. A. T.; Pez, G. P. *Chem. Commun.* **1991**, 971–972. (c) Gardiner, R.; Brown, D. W.; Kirlin, P. S.; Rheingold, A. L. *Chem. Mater.* **1991**, *3*, 1053–1059. (d) Drake, S. R.; Hursthouse, M. B.; Abdul Malik, K. M.; Miller, S. A. S. *Inorg. Chem.* **1993**, *32*, 4653–4657. (e) Neumayer, D. A.; Studebaker, D. B.; Hinds, B. J.; Stern, C. L.; Marks, T. J. *Chem. Mater.* **1994**, *6*, 878–880. (f) Tobaly, P.; Watson, I. M. *J. Chem. Thermodynamics* **1995**, *27*, 1211–1219. (g) Igumenov, I. K.; Semyannikov, P. P.; Belaya, S. V.; Zanina, A. S.; Shergina, S. I.; Sokolov, I. E. *Polyhedron* **1996**, *15*, 4521–4530. (h) Belot, J. A.; Neumayer, D. A.; Reedy, C. J.; Studebaker, D. B.; Hinds, B. J.; Stern, C. L.; Marks, T. J. *Chem. Mater.* **1997**, *9*, 1638–1648. (i) Teren, A. R.; Belot, J. A.; Edleman, N. L.; Marks, T. J.; Wessels, B. W. *Chem. Vap. Deposition* **2000**, *6*, 175–177. (j) Marks, T. J.; Belot, J. A.; Reedy, C. J.; McNeely, R. J.; Studebaker, D. B.; Neumayer, D. A.; Stern, C. L. *J. Alloys Compd.* **1997**, *251*, 243–248.

(12) Otway, D. J.; Rees, W. S.Jr. *Coord. Chem. Rev.* **2000**, *210*, 279–328.

(13) Selected examples: (a) Schulz, D. L.; Hinds, B. J.; Stern, C. L.; Marks, T. J. *Inorg. Chem.* **1993**, *32*, 249–250. (b) Schulz, D. L.; Hinds, B. J.; Neumayer, D. A.; Stern, C. L.; Marks, T. J. *Chem. Mater.* **1993**, *5*, 1605–1617. (c) Neumayer, D. A.; Belot, J. A.; Feezel, R. L.; Reedy, C.; Stern, C. L.; Marks, T. J. *Inorg. Chem.* **1998**, *37*, 5625–5633.

(14) El-Kaderi, H. M.; Heeg, M. J.; Winter, C. H. *Organometallics* **2004**, *23*, 4995–5002.

(15) (a) Rees, W. S.Jr.; Moreno, D. A. *Chem. Commun.* **1991**, *24*, 1759–1760. (b) Hermann, W. A.; Huber, N. W.; Priermeier, T. *Angew. Chem., Int. Ed. Engl.* **1994**, *33*, 105–107. (c) Chi, Y.; Ranjan, S.; Chou, T.; Liu, C.; Peng, S.; Lee, G. *Dalton Trans.* **2001**, 2462–2466.

(16) (a) Hitzbleck, J.; O'Brien, A. Y.; Forsyth, C. M.; Deacon, G. B.; Ruhlandt-Senge, K. *Chem.—Eur. J.* **2004**, *10*, 3315–3323. (b) El-Kaderi, H. M.; Heeg, M. J.; Winter, C. H. *Polyhedron* **2005**, 645–653. (c) El-Kaderi, H. M.; Heeg, M. J.; Winter, C. H. *Eur. J. Inorg. Chem.* **2005**, 2081–2088. (d) Hitzbleck, J.; O'Brien, A. Y.; Forsyth, C. M.; Deacon, G. B.; Ruhlandt-Senge, K. *Inorg. Chem.* **2006**, *45*, 10329–10337. (e) Hitzbleck, J.; Deacon, G. B.; Ruhlandt-Senge, K. *Angew. Chem., Int. Ed.* **2004**, *43*, 5218–5220.

(17) For reviews see: (a) Hanusa, T. P. *Chem. Rev.* **1993**, *93*, 1023–1036. (b) Hanusa, T. P. *Organometallics* **2002**, *21*, 2559–2571.

(18) (a) Li, W.-M.; Ritala, M.; Leskelä, M.; Lappalainen, R.; Jokinen, J.; Soininen, E.; Hüttl, B.; Nykänen, E.; Niinistö, L. *J. Appl. Phys.* **1998**, *84*, 1029–1035. (b) Soininen, P.; Niinistö, L.; Nykänen, E.; Leskelä, M. *Appl. Surf. Sci.* **1994**, *75*, 99–105.

(19) For selected examples, see: (a) Drake, S. R.; Hursthouse, M. B.; Malik, K. M. A.; Otway, D. J. *J. Chem. Soc., Dalton Trans.* **1993**, 2883–2890. (b) Rossetto, G.; Polo, A.; Benetollo, F.; Porcha, M.; Zanella, P. *Polyhedron* **1992**, *11*, 979–985. (c) Drozdov, A. A.; Trojanov, S. I. *Polyhedron* **1992**, *11*, 2877–2882.

(20) (a) Lee, S. W.; Kwon, O. S.; Hwang, C. S. *Microelectron. Eng.* **2005**, *80*, 158–161. (b) Kwon, O. S.; Kim, S. K.; Cho, M.; Hwang, C. S.; Jeong, J. *J. Electrochem. Soc.* **2005**, *152*, C229–C236. (c) Kil, D.-S.; Lee, J.-M.; Roh, J.-S. *Chem. Vap. Deposition* **2002**, *8*, 195–197.

(21) (a) Hatanpää, T.; Ritala, M.; Leskelä, M. *J. Organomet. Chem.* **2007**, *692*, 5256–5262. (b) Vehkamäki, M.; Hatanpää, T.; Ritala, M.; Leskelä, M.; Väyrynen, S.; Rauhala, E. *Chem. Vap. Deposition* **2007**, *13*, 239–246. (c) Kukli, K.; Ritala, M.; Sajavaara, T.; Hänninen, T.; Leskelä, M. *Thin Solid Films* **2006**, *500*, 322–329. (d) Hatanpää, T.; Vehkamäki, M.; Mutikainen, I.; Kansikas, J.; Ritala, M.; Leskelä, M. *Dalton Trans.* **2004**, 1181–1190. (e) Vehkamäki, M.; Hänninen, T.; Ritala, M.; Leskelä, M.; Sajavaara, T.; Rauhala, E.; Keinonen, J. *Chem. Vap. Deposition* **2001**, *7*, 75–80. (f) Vehkamäki, M.; Hatanpää, T.; Hänninen, T.; Ritala, M.; Leskelä, M. *Electrochem. Solid-State Lett.* **1999**, *2*, 504–506.

(22) Dezelah, C. L.IV; Wiedmann, M. K.; Mizohata, K.; Baird, R. J.; Niinistö, L.; Winter, C. H. *J. Am. Chem. Soc.* **2007**, *129*, 12370–12371.

(23) For reviews see: (a) Trofimenko, S. *Chem. Rev.* **1993**, *93*, 943–980. (b) Trofimenko, S. *Scorpionates-The Coordination Chemistry of Polypyrazolylborate Ligands*; Imperial College Press: London, 1999.

(24) Trofimenko, S. *J. Am. Chem. Soc.* **1967**, *89*, 3170–3177.

complexes (sublime ~200 °C/10^{-3} Torr); however, investigation into their thermal stability and volatility was minimal.[25a−25d] Recently, the deposition of β-BaB_2O_4 thin films by CVD was reported using barium tris(pyrazolyl)borate ("BaTp$_2$") as the source compound, and thermogravimetric analyses suggested that "BaTp$_2$" exhibits good thermal stability.[8c]

Herein, we describe the synthesis, structure, and properties of a series of homoleptic calcium, strontium, and barium complexes containing various substituted tris(pyrazolyl)borate ligands. With the exception of [BaTp$_2$]$_2$, the compounds documented herein exhibit good volatility and exceptional thermal stability, and many melt at temperatures below those required for vapor transport. These new complexes thus represent a breakthrough in precursor design for CVD and especially ALD growth of thin films containing the heavier group 2 elements.

Results

Synthetic Aspects. The complexes SrTp$_2$ (**1**),[24] "BaTp$_2$" ([BaTp$_2$]$_2$, **2**),[24] SrTp$_2^{Me2}$ (**3**),[25d] and BaTp$_2^{Me2}$ (**4**)[25d] were prepared according to literature procedures. Access to analogues containing other 3,5-dialkyl-substituted Tp ligands required synthesis of the corresponding potassium salts, which have not been previously reported. These salts were prepared by heating a solid mixture of potassium borohydride with a slight excess of either 3,5-diethylpyrazole or 3,5-di-*n*-propylpyrazole at temperatures between 180 and 190 °C, followed by precipitation with hexane, to afford white powders of potassium tris(3,5-diethylpyrazolyl)borate (KTp^{Et2}, 61%) and potassium tris(3,5-di-*n*-propylpyrazolyl)borate (KTp^{nPr2}, 31%) after workup (eq 1). KTp^{Et2} and KTp^{nPr2} are very soluble in THF and toluene. KTp^{nPr2} is also slightly soluble in hexane, which led to the low isolated yield. The compositions were verified by spectroscopic and analytical methods. Characteristic bands for the boron−hydrogen stretch at 2444 cm^{-1} and for the carbon−nitrogen stretch at 1533 cm^{-1} were found in the infrared spectra of both compounds. The ^{1}H NMR spectra for KTp^{Et2} showed a resonance for the 4-hydrogen atom of the pyrazolyl group at δ 5.82, as well as resonances belonging to two magnetically inequivalent ethyl groups. Similarly, the ^{1}H NMR spectra for KTp^{nPr2} contained a resonance at δ 5.77 belonging to the 4-hydrogen atom of the pyrazolyl group, and resonances corresponding to two magnetically inequivalent *n*-propyl groups.

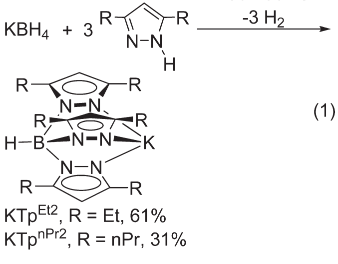

KTp^{Et2}, R = Et, 61%
KTp^{nPr2}, R = nPr, 31%

(1)

Treatment of MI_2 (M = Ca, Sr) or $BaI_2(THF)_3$ with 2 equiv of KTp^{Et2} or KTp^{nPr2} yielded **5**−**10** in good to moderate yields (eq 2). Complexes **5**−**7** are soluble in hexane, from which colorless crystals suitable for X-ray crystallography were grown at −23 °C. Complexes **8**−**10** are very soluble in hexane and increase in solubility in going from the calcium derivative **8** to the barium complex **10**. Complexes **8** and **9** exist as colorless crystalline solids, whereas **10** is a colorless, greasy solid. Samples of **1**−**10** for microanalyses were obtained by preparative sublimations at 0.05 Torr.

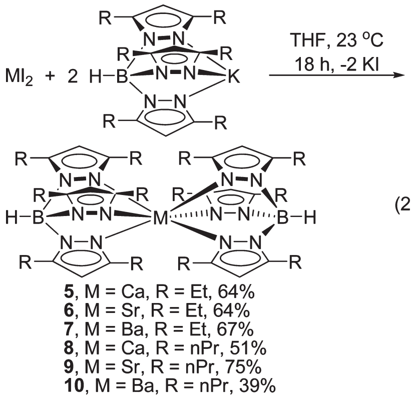

5, M = Ca, R = Et, 64%
6, M = Sr, R = Et, 64%
7, M = Ba, R = Et, 67%
8, M = Ca, R = nPr, 51%
9, M = Sr, R = nPr, 75%
10, M = Ba, R = nPr, 39%

(2)

The compositions of **1**, **2**, and **5**−**10** were assessed by ^{1}H NMR and $^{13}C\{^1H\}$ NMR spectroscopy, infrared spectroscopy, and C, H, N microanalyses. As detailed below, **1** and **5**−**10** exist as six-coordinate mononuclear complexes containing two tridentate tris(pyrazolyl)borate ligands, whereas **2** exists as an eight-coordinate dinuclear complex composed of two terminal and two bridging Tp ligands. Complexes **1** and **2** were originally reported by Trofimenko,[24] but X-ray crystallographic analyses have not been previously reported for either complex. Malandrino suggested that **2** possessed a monomeric structure, based upon observation of a molecular ion in the fast atom bombardment mass spectrum and lack of higher mass peaks.[8c] The present work clearly demonstrates a dimeric solid state structure for **2**. Malandrino also reported a melting point of 300 °C for **2** from differential scanning calorimetry.[8c] In the present work, multiple determinations on sublimed samples of **2** revealed a consistent melting point of 250−252 °C. Complexes **1** and **2** both have a boron−hydrogen infrared stretching frequency of 2529 cm^{-1}. The boron−hydrogen infrared stretches in **5**−**7** and **8**−**10** fall in the range of 2526−2532 cm^{-1} and 2470−2517 cm^{-1}, respectively, with no notable trend upon increasing ionic size from calcium, strontium, to barium. The ^{1}H NMR and $^{13}C\{^1H\}$ NMR spectra of **1** and **2** at 23 °C are similar to each other, with resonances belonging to three different protons and carbon atoms from the pyrazolyl rings. The ^{1}H NMR and $^{13}C\{^1H\}$ NMR spectra for **5**−**7** and **8**−**10** are similar to the spectra for KTp^{Et2} and KTp^{nPr2}, respectively. In the ^{1}H NMR spectra of **1**−**10**, the boron-bound hydrogen atoms resonated as a very broad singlet between δ 4.7 and 5.0.

To gain insight into the solution structure of **2**, ^{1}H NMR spectra were recorded in toluene-d_8 at room temperature and −80 °C. The ^{1}H NMR spectrum at room temperature showed a triplet at δ 5.97, corresponding to the hydrogen atom at the 4-position of the pyrazolyl groups, and two doublets at δ 7.57 and 7.03 belonging to the hydrogen atoms at the 3- and 5-positions of the pyrazolyl groups. The ^{1}H NMR spectrum at −80 °C had a total of six equal intensity resonances corresponding to two inequivalent Tp ligands (δ 7.76, 7.40, 7.29, 6.61, 6.07, 5.81). These resonances are consistent with the terminal and bridging Tp ligands in the dimeric structure of **2** (see below) and further suggest that the bridging pyrazolyl groups are undergoing site exchange rapidly at −80 °C.

Volatility and Thermodynamic Stability Study. Compounds **1**−**10** were studied by melting point and decomposition determinations, preparative sublimations, and thermogravimetric analysis (TGA) to assess their initial suitability as ALD and CVD precursors. The data for **1**−**10** are summarized in Table 6. Careful decomposition temperatures were determined using a melting point apparatus with sealed capillary tubes containing a few milligrams of **1**−**10**, as described in the Experimental Section. The calcium complexes **5** and **8** do not decompose below 400 °C. Strontium complexes **1** and **3** decompose at 363 and 380 °C, respectively, whereas the higher alkyl-substituted derivatives **6** and **9** show no evidence for decomposition up to 400 °C. The barium complexes **2**, **4**, **7**, and **10** decompose between 330 and 380 °C, and the thermal stability increases with increasing size of the groups at the 3- and 5-positions of the tris(pyrazolyl)borate ligands. The decomposition temperature of **2** (330 °C) was the lowest among **1**−**10**, probably because of its dimeric structure. Purified solids of **1**−**10** were carefully sublimed at 0.05 Torr on a preparative scale (0.5−1.0 g), as described in the experimental section, to assess volatility and thermal stability during vapor transport. Complex **1** is the most volatile among **1**−**10** and sublimes at 200 °C with a sublimed recovery of 99.3% and a residue of 0.1%. Complexes **3** and **8**−**10** are the least volatile of the series, with sublimation temperatures of 240 °C. Significantly, **8**−**10** melt before sublimation (mp **8** = 169−172 °C, mp **9** = 164−168 °C, mp **10** = 141−144 °C) and therefore sublime from liquids. Complexes **4** and **5**−**7** sublime between 210 and 220 °C, and **6** and **7** volatilize as liquids (mp **6** = 188−190 °C, mp **7** = 129−131 °C). The sublimed recoveries for **5**−**9** are ≥99.0%, with corresponding nonvolatile residues of <1%. Complexes **4** and **10** have sublimed recoveries of 91.4 and 97.7%, with nonvolatile residues of 0.4 and 2.1%, respectively. Complexes **2** and **3** have low sublimed recoveries of 78.4 and 85.5%, with nonvolatile residues of 17.3 and 7.3%, respectively.

The TGA traces for **1**−**4** are shown in Chart 1. Complexes **1** and **2** show a single sublimation step from 248 to 354 °C and 301−420 °C with residues of 9.5 and 46.5%, respectively. The TGA traces for **3** and **4** exhibit a single sublimation step from 325 to 409 °C and 287−394 °C, respectively, and both show residues of 3.6%. Chart 2 contains the TGA traces for **5**−**10**. Weight loss for **5** occurs between 277 and 387 °C, with a residue of 0.1%. The TGA traces for **6** and **7** are similar and reveal a single sublimation step from 299 to 398 °C, with residues of 2.4 and 1.1%, respectively. Complexes **8**−**10** have very similar TGA traces composed of single sublimation steps from 298 to 420 °C, with residues of 2.2, 1.5, and 5.5%, respectively.

Chart 1. TGA Traces for **1**−**4** from 200 to 450 at 10 °C/min

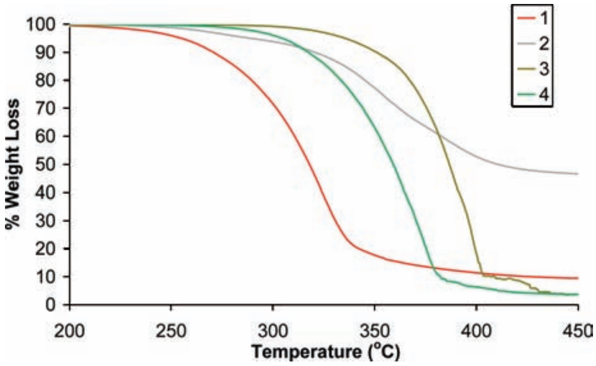

Chart 2. TGA Traces for **5**−**10** from 200 to 450 at 10 °C/min

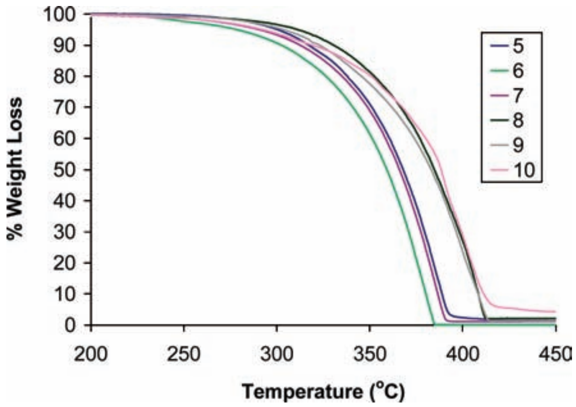

Structural Aspects. The X-ray crystal structures of **1**, **2**, and **5**−**7** were determined to establish the geometries about the metal centers and the bonding modes of the Tp and Tp^{Et2} ligands. Experimental crystallographic data are summarized in Table 1, selected bond lengths and angles are given in Tables 2−5, and perspective views are presented in Figures 1−5. The X-ray crystal structures of **3** and **4** have been previously reported.[25a−25d] A low precision X-ray crystal structure determination of **9** revealed a monomeric formulation with a molecular structure similar to that of **6**. Single crystals of **8** and **10** with sufficient quality for X-ray crystal structure determinations could not be grown, despite many attempts. The molecular structures of **8** and **10** are presumably comparable to those of **5**, **7**, and **9**.

The molecular structures of **1**, **5**, and **6** are similar and their perspective views are shown in Figures 1, 3, and 4. The unit cell of **1** contains two crystallographically independent molecules that exhibit identical metrical parameters within experimental uncertainty. As such, only data for the molecule containing Sr(1) will be discussed herein. Molecules of **1**, **5**, and **6** exist as mononuclear complexes with two Tp or Tp^{Et2} ligands coordinated to the metal center in a tridentate fashion through the nitrogen atoms. The three pyrazolyl moieties on the two Tp and Tp^{Et2} ligands are arrayed in a staggered conformation, affording distorted octahedral geometry. The average strontium−nitrogen bond lengths for **1** and **6** are 2.593(15) and 2.606(9) Å, respectively, which are within experimental error of each other, as well as with the strontium−nitrogen bond lengths in **3** (avg = 2.597 (6) Å).[25b] The average calcium−nitrogen bond length in **5** is 2.459(6) Å and is similar to those of CaTp$_2$ (avg = 2.44(2) Å)[25e] and CaTp$_2^{Me2}$ (2.454(2) Å).[25b] The boron−metal−boron′ bond angles are 180° for **1**, **5**, and **6**.

Table 1. Crystal Data and Data Collection Parameters for **1**, **2**, and **5**−**7**

	1	**2**	**5**	**6**	**7**
formula	$C_{18}H_{20}B_2N_{12}Sr$	$C_{36}H_{40}B_4Ba_2N_{24}$	$C_{42}H_{68}B_2CaN_{12}$	$C_{42}H_{68}B_2SrN_{12}$	$C_{42}H_{68}B_2BaN_{12}$
FW	513.70	1126.84	802.78	850.32	900.04
space group	$P2(1)/c$	$C2/c$	$P2(1)/n$	$P2(1)/n$	$P2(1)/n$
a (Å)	13.4182(4)	19.8850(11)	11.0949(4)	11.3183(2)	17.2512(5)
b (Å)	14.8732(4)	15.9199(11)	12.5709(4)	12.5687(3)	12.9047(4)
c (Å)	11.7611(3)	16.6548(13)	16.6206(6)	16.4972(4)	21.9773(6)
β	94.8380(10)	119.481(4)	106.084(2)	106.2430(10)	111.670(2)
V (Å^3)	2338.82(11)	4589.7(5)	2227.38(13)	2253.15(9)	4546.8(2)
Z	4	4	2	2	4
T (K)	100(2)	100(2)	100(2)	100(2)	100(2)
λ (Å)	0.71073	0.71073	0.71073	0.71073	0.71073
ρ_{calcd} (g, cm^{-3})	1.459	1.631	1.197	1.253	1.315
μ (mm^{-1})	2.338	1.764	0.185	1.240	0.917
R(F)(%)^a	5.74	2.48	7.67	5.07	3.54
Rw(F)(%)^a	13.33	5.82	20.24	13.23	8.32

[a] $R(F) = \sum||F_o| - |F_c||/\sum|F_o|$, $Rw(F)^2 = [\sum w(F_o^2 - F_c^2)^2/\sum w(F_o^2)^2]^{1/2}$ for $I > 2\sigma(I)$.

Table 2. Selected Bond Lengths (Å) and Angles (deg) for **1**

Sr(1)−N(1)	2.585(4)
Sr(1)−N(3)	2.610(4)
Sr(1)−N(5)	2.584(4)
N(1)−Sr(1)−N(1)′	180
N(1)−Sr(1)−N(3)	77.16(12)
N(1)−Sr(1)−N(3)′	102.84(12)
N(1)−Sr(1)−N(5)	78.42(13)
N(1)−Sr(1)−N(5)′	101.58(13)
N(3)−Sr(1)−N(3)′	180
N(3)−Sr(1)−N(5)	71.23(13)
N(3)−Sr(1)−N(5)′	108.77(13)
N(5)−Sr(1)−N(5)′	180

Table 3. Selected Bond Lengths (Å) and Angles (deg) for **2**^{a}

Ba(1)−N(1)	2.829(1)
Ba(1)−N(3)	2.785(1)
Ba(1)−N(5)	2.880(3)
Ba(1)−N(5)′	2.760(4)
Ba(1)−N(7)	2.820(1)
Ba(1)−N(9)	3.087(1)
Ba(1)−N(9)′	2.941(1)
Ba(1)−N(10)	3.211(1)
Ba(1)−N(12)′	2.821(1)
Ba(1)−C(13)	3.173(3)
Ba(1)−C(14)	3.379(2)
Ba(1)−C(15)	3.400(1)
N(1)−Ba(1)−N(3)	68.42(4)
N(1)−Ba(1)−N(5)′	70.67(8)
N(1)−Ba(1)−N(5)	67.40(7)
N(3)−Ba(1)−N(5)′	73.10(8)
N(3)−Ba(1)−N(5)	66.93(7)

[a] The atoms N(5)′, N(6)′, C(7)′, C(8)′, C(9)′, and B(1)′ are part of an alternate set of positions describing a 50/50 disorder. Other primed designations (N(5)′, N(9)′, and N(12)′) reflect symmetry related positions.

Table 4. Selected Bond Lengths (Å) and Angles (deg) for **5** and **6**

	5	**6**
M−N(1)	2.465(2)	2.615(2)
M−N(3)	2.460(2)	2.606(2)
M−N(5)	2.453(2)	2.598(2)
N(1)−M−N(1)′	180	180
N(1)−M−N(3)	79.17(7)	75.34(6)
N(1)−M−N(3)′	100.83(7)	104.66(6)
N(1)−M−N(5)	79.49(7)	74.67(6)
N(1)−M−N(5)′	100.51(7)	105.33(6)
N(3)−M−N(3)′	180	180
N(3)−M(1)−N(5)	78.07(8)	73.43(6)
N(3)−M(1)−N(5)′	101.93(8)	106.57(6)
N(5)−M(1)−N(5)′	180	180

Table 5. Selected Bond Lengths (Å) and Angles (deg) for **7**

Ba−N(1)	2.769(2)
Ba−N(3)	2.781(2)
Ba−N(5)	2.789(2)
Ba−N(7)	2.759(2)
Ba−N(9)	2.816(2)
Ba−N(11)	2.751(2)
N(1)−Ba−N(3)	70.24(5)
N(1)−Ba−N(5)	72.98(5)
N(1)−Ba−N(7)	100.85(5)
N(1)−Ba−N(9)	111.77(5)
N(1)−Ba−N(11)	168.54(6)
N(3)−Ba−N(5)	68.47(6)
N(3)−Ba−N(7)	95.35(6)
N(3)−Ba−N(9)	164.22(6)
N(3)−Ba−N(11)	102.23(6)
N(5)−Ba−N(7)	163.75(6)
N(5)−Ba−N(9)	127.32(6)
N(5)−Ba−N(11)	112.96(5)
N(7)−Ba−N(9)	68.87(6)
N(7)−Ba−N(11)	70.71(6)
N(9)−Ba−N(11)	73.05(6)

A perspective view of **7** is shown in Figure 5. Overall, the structure of **7** is similar to those of **5** and **6** in that it has two Tp^{Et2} ligands with distorted octahedral geometry. The barium−nitrogen bond distances in **7** range between 2.751(2) and 2.816(2) Å (avg = 2.78(2) Å), which are similar to the values previously reported for **4** (avg = 2.760(1),[25a] 2.754(3) Å[25d]). Unlike **1**, **5**, and **6**, the boron−barium−boron′ angle in **7** is bent (165.1(1)°). Interestingly, the boron−nitrogen−nitrogen and nitrogen−boron−nitrogen bond angles are virtually identical for **5**−**7**, even though the ionic size of the metal increases through the series and **7** additionally adopts a bent conformation.

A perspective view of **2** is shown in Figure 2. The molecular structure of **2** consists of a dinuclear complex with two $BaTp_2$ units related by a center of inversion. Each barium ion contains a terminally bound Tp ligand coordinated in a tridentate fashion. The metal ions are held together by two symmetrical Tp ligands, which involve one pyrazolyl moiety bonding in an η^5-fashion to one barium ion, and the same pyrazolyl ring bonding η^1 to the other barium ion. The other two pyrazolyl moieties bridge the metal centers, with each one binding in an η^1-fashion through the lone pairs on the nitrogen atoms. The barium−nitrogen distances in the terminal

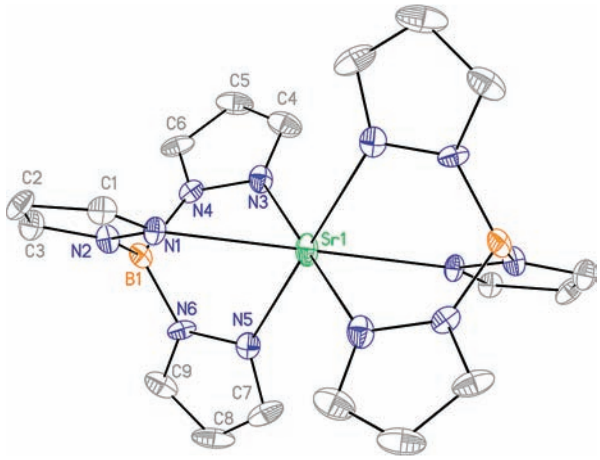

Figure 1. Perspective view of **1** with thermal ellipsoids at the 50% probability level.

Table 6. Preparative Sublimation Data and Decomposition Temperatures for **1**−**10**[a]

compound	sublimation temperature (°C/0.05 Torr)	% ecovery	% residue	decomposition temperature (°C)
1	200	99.3	0.1	~363
2	220	78.4	17.3	~330
3	240	85.5	7.3	~380
4	220	91.4	0.4	~350
5	210	99.3	0.2	>400
6	210	99.0	0.1	>400
7	215	99.0	0.8	~380
8	240	99.3	0.2	>400
9	240	99.1	0.6	>400
10	240	97.7	2.1	~380

[a] All sublimations were carried out on a 0.5−1.0 g scale, and were complete within 3−5 h.

Tp ligands range from 2.760(4)−2.880(3) Å (avg. = 2.81(5) Å), which are longer than the barium−nitrogen distances in **4** and **7**. This elongation is likely related to a higher coordination number of eight for **2**, versus only six for **4** and **7**. The Ba−N(7) and Ba−N(12)′ bond lengths are 2.820(1) Å and 2.821(1) Å, respectively. The Ba−N(9)′ bond length is 2.941(1) Å, which is quite long compared to the σ-interactions in the terminal and bridging Tp ligands. The boron−nitrogen−nitrogen and nitrogen−boron−nitrogen bond angles range from 120.71(11)−125.06(17) and 105.0(2)−122.9(3)°, respectively. These large ranges illustrate the flexibility of the Tp ligand. The average carbon−nitrogen, carbon−carbon, and nitrogen−nitrogen bond lengths in the η^1-pyrazolyl rings are 1.346(5) Å, 1.383(5) Å, and 1.364(5) Å, respectively. These values are consistent with delocalized bonding and compare well with those of **1** ($C-N_{avg}$ = 1.346(10), $C-C_{avg}$ = 1.381(15), N−N = 1.364(9) Å). The bond distances inside the η^5-pyrazolyl ring (N(9)−C(13) = 1.344(2) Å, C(13)−C(14) = 1.400(2) Å, C(14)−C(15) = 1.384(2) Å, C(15)−N(10) = 1.356(2) Å, N(10)−N(9) = 1.369(1) Å) are within experimental error of the values in the η^1-pyrazolyl moieties in **2** and the pyrazolyl rings in **1**. Therefore, the η^5-pyrazolyl group π-cloud is not significantly perturbed by coordination to the barium ion.

Discussion

This work documents the combination of exceptional thermal stability and reasonable volatility in **1**−**10**. The barium precursors **7** and **10** decompose in the solid state at about 375 °C, whereas the calcium and strontium complexes **5**, **6**, **8**, and **9** decompose at >400 °C. The high thermal stability of **5**−**10** is further supported by the excellent recoveries in the preparative sublimation studies and low residues observed in the TGA traces. The higher thermal stability of **5**−**10**, compared to analogues **1**−**4**, is probably related to kinetic protection of the electron-rich B−H moieties and metal centers by the ethyl and *n*-propyl groups. A pervasive problem in the CVD growth of films containing the heavier group 2 elements is premature or concurrent precursor thermal decomposition during vapor transport.[1] The exceptional thermal stability of **5**−**10**, as described herein, eliminates the issue of solid state decomposition during vapor transport. In addition, ALD growth requires that a precursor be thermally stable at the film growth temperature to avoid loss of the self-limited growth mechanism and emergence of CVD-like growth.[10] We have previously observed that the upper temperature range of self-limited growth corresponds closely to the solid state decomposition temperatures of several metalorganic ALD precursors.[26] As such, use of **7** and **10** in ALD growth may allow self-limited ALD growth up to about 375 °C, and to >400 °C for **5**, **6**, **8**, and **9**. To our knowledge, **5**−**10** are the most stable thermally stable heavier group 2 metalorganic precursors available to date. Among **1**−**10**, **5**−**7** sublime with <1% nonvolatile residues between 210 and 215 °C/0.05 Torr and have the highest thermal stabilities for each metal. In addition, **6**−**8** melt prior to vaporization, and thus undergo vapor transport from liquids. Precursors that undergo vapor transport from liquids are highly desirable, since they avoid particles from solid precursors and facilitate steady vapor transport because of the relatively constant surface area of a liquid, compared to irregular vapor transport from solid precursors with changing surface areas. As such, **6**−**8** have the best film growth precursor properties in the series. In addition, **6**−**8** are solids at ambient temperature and are air and water stable, which allows convenient laboratory manipulation.

Malandrino has reported the use of "$BaTp_2$" (**2**) as a CVD precursor for the growth of BaB_2O_4 films and also showed that this compound exhibited a single weight loss event in the TGA trace with a nonvolatile residue of 9% at 340 °C.[8c] As documented herein, **2** possesses the poorest precursor properties among **1**−**10**: it sublimes slowly at 220 °C/0.05 Torr, leaves a 17.3% nonvolatile residue after sublimation, decomposes at about 330 °C in the solid state, and afforded a 45.6% nonvolatile residue in the TGA trace after heating to 450 °C. The poor precursor characteristics of **2** are clearly related to its dimeric solid state structure.

---

(25) (a) Dutremez, S. G.; Leslie, D. B.; Streib, W. E.; Chisholm, M. H.; Caulton, K. G. *J. Organomet. Chem.* **1993**, *462*, C1–C2. (b) Sohrin, Y.; Matsui, M.; Hata, Y.; Hasegawa, H.; Kokusen, H. *Inorg. Chem.* **1994**, *33*, 4376–4383. (c) Belderraín, T. R.; Contreras, L.; Paneque, M.; Carmona, E. *J. Organomet. Chem.* **1994**, *474*, C5–C7. (d) Belderraín, T. R.; Contreras, L.; Paneque, M.; Carmona, E.; Monge, A.; Ruiz, C. *Polyhedron* **1996**, *15*, 3453–3463. (e) Sohrin, Y.; Kokusen, H.; Kihara, S.; Matsui, M.; Kushi, Y.; Shiro, M. *J. Am. Chem. Soc.* **1993**, *115*, 4128–4136.

(26) (a) Dezelah, C. L.IV; El-Kadri, O. M.; Szilágyi, I.; Campbell, J. M.; Arstila, K.; Niinistö, L.; Winter, C. H. *J. Am. Chem. Soc.* **2006**, *128*, 9638–9639. (b) Dezelah, C. L.IV; El-Kadri, O. M.; Kukli, K.; Arstila, K.; Baird, R. J.; Lu, J.; Niinistö, L.; Winter, C. H. *J. Mater. Chem.* **2007**, *17*, 1109–1116.

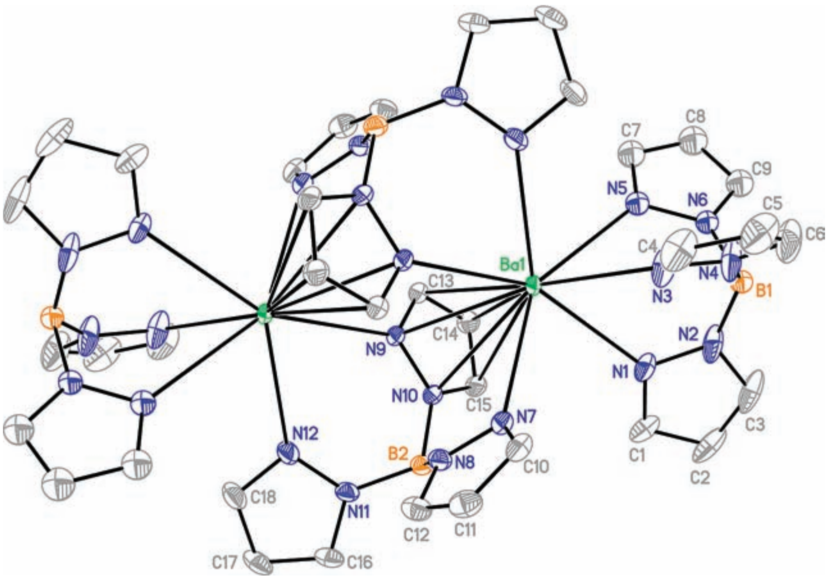

Figure 2. Perspective view of **2** with thermal ellipsoids at the 50% probability level.

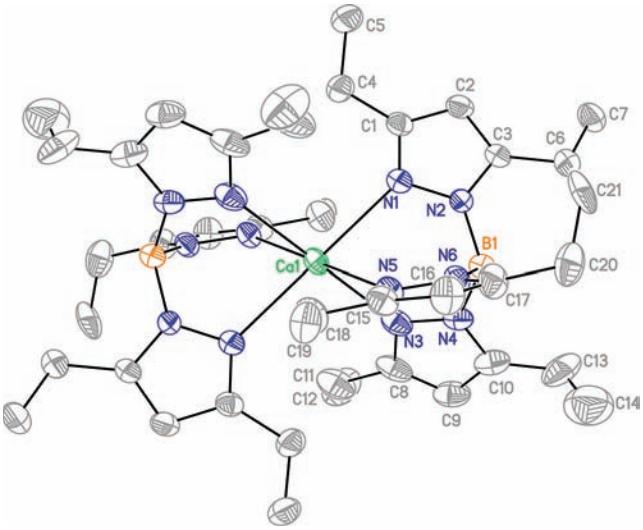

Figure 3. Perspective view of **5** with thermal ellipsoids at the 50% probability level.

The molecular structure of **2** contains an η^5-pyrazolyl-barium interaction and is the first example of such a bonding mode in a group 2 tris(pyrazolyl)borate complex. Examples of η^5-pyrazolyl interactions with group 1 metal ions have been documented in $KTp^{CF3,CH3}$ ($KTp^{CF3,CH3}$ = hydrotris (3-trifluoromethyl-5-methylpyrazolyl)borate) and KLL_2' (L = tris[3-(2-methoxy-1,1-dimethylethyl)pyrazolyl]borate, L′ = 3-(2-methoxy-1,1-dimethylethyl)pyrazole).[27,28] Stalke and co-workers[29] reported the X-ray crystal structure of $Ba[(Pz^*)_3Ge]_2 \cdot (dioxane)_{0.5}$ (Pz* = 3,5-dimethylpyrazolyl), in which two of the six Pz* moieties are coordinated to the barium ions in an η^4-fashion. The remaining Pz* ligands bond to the barium ions with conventional σ-bonds through the 2-nitrogen atoms. The Ba−N(9) and Ba−N(10) distances within the η^5-pyrazolyl-barium interaction in **2** are 3.087(1) Å and 3.211(1) Å, respectively, which are longer than the average π-bonded barium−nitrogen distances in $Ba[(Pz^*)_3Ge]_2 \cdot (dioxane)_{0.5}$ (2.947 Å). The average barium−carbon

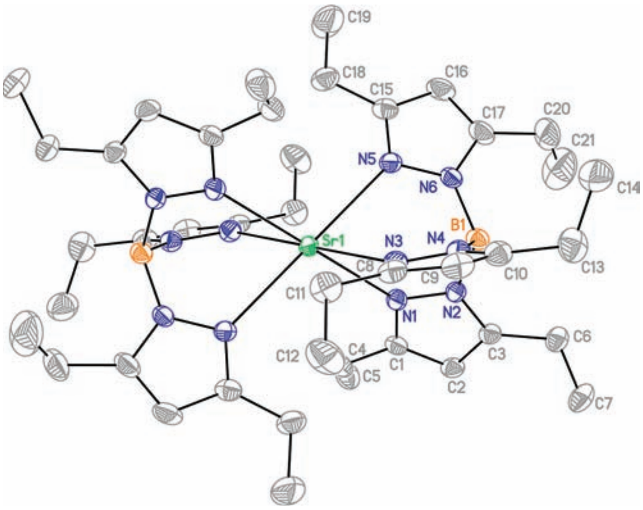

Figure 4. Perspective view of **6** with thermal ellipsoids at the 50% probability level.

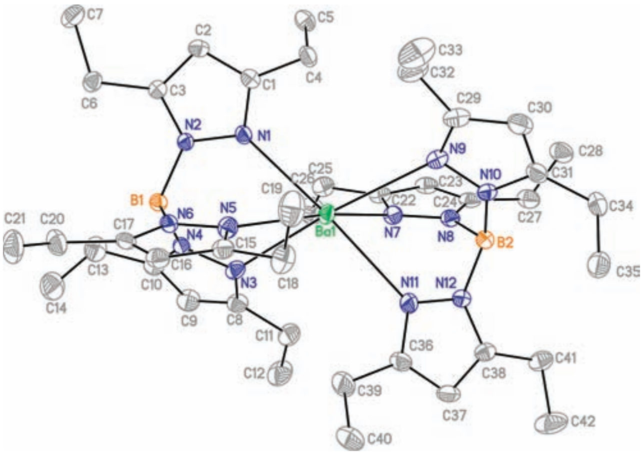

Figure 5. Perspective view of **7** with thermal ellipsoids at the 50% probability level.

---

(27) Hu, Z.; Gorun, M. *Inorg. Chem.* **2001**, *40*, 667–671.

(28) Chisholm, M. H.; Gallucci, J. C.; Yaman, G. *Chem. Commun.* **2006**, 1872–1874.

(29) Steiner, A.; Stalke, D. *Inorg. Chem.* **1995**, *34*, 4846–4853.

Table 7. Comparison of the Average Metal−Nitrogen Bond Lengths (Å), Average cis Nitrogen−Metal−Nitrogen′ (deg) Intraligand Bond Angles, Average cis Nitrogen−Metal−Nitrogen Interligand Bond Angles (deg), Average Boron−Nitrogen−Nitrogen Angles (deg), and Average Nitrogen−Boron−Nitrogen Angles (deg) for **5**−**7**

Complex	M−N	$N-M-N_{intraligand}$	$N-M-N'_{interligand}$	B−N−N	N−B−N
5	2.459(6)	78.9(8)	101.1(7)	121.9(4)	110.6(6)
6	2.606(9)	74.5(1)	105.5(1)	122.1(6)	110.8(5)
7	2.78(2)	71(2)	108(11)	122.2(5)	111.3(6)

contacts in $Ba[(Pz^*)_3Ge]_2 \cdot (dioxane)_{0.5}$ are 3.334 Å and compare well with the related values in **2** (3.173(1)−3.400(1), avg = 3.318 (5) Å). Metallocenes such as $Ba(C_5Me_5)_2$,[30] $Ba(C_5H(C_3H_7)_4)_2$,[31] and $Ba(C_5H_3(SiMe_3)_2)_2$[32] have average barium−carbon bond distances of 2.98(1), 2.94(1), and 3.01(2) Å, respectively, which are shorter than the barium−carbon distances in **2**. These differences reflect the anionic nature of the cyclopentadienyl ligands, the more neutral ligand character of the pyrazolyl groups in **2**, as well as the higher coordination number in **2** compared to the barocenes.

A summary of important structural parameters for **5**−**7** is shown in Table 7. As the metal ion radius increases, the average cis nitrogen−metal−nitrogen intraligand bond angle decreases and the average nitrogen−metal−nitrogen′ interligand bond angle increases. In addition, the average boron−nitrogen−nitrogen and nitrogen−boron−nitrogen angles are the same within experimental uncertainty in **5**−**7**, which suggests that the cavity size of the Tp^{Et2} ligand does not change even though the size of the metal ion increases. The constant cavity size is attributed to the 5-ethyl groups of the pyrazolyl moieties, which interact sterically with the boron−hydrogen fragment and prevent the boron−nitrogen−nitrogen angle from expanding. Since the metal−nitrogen distances increase while the cavity size remains the same, the average nitrogen−metal−nitrogen intraligand bond angle decreases and the average nitrogen−metal−nitrogen′ interligand angle increases. Belderraín and coworkers[25d] made a similar correlation by comparing the nitrogen−metal−nitrogen intraligand bond angle and nitrogen−metal−nitrogen′ interligand angle for MTp_2^{Me2} (M = Mg, Ca, Sr, Ba). It is not surprising that the Tp^{Me2} and Tp^{Et2} ligands have very similar structural parameters with respect to the nitrogen−metal−nitrogen intraligand and nitrogen−metal−nitrogen′ interligand angles, since the steric profiles of methyl and ethyl groups are similar. As previously noted, the boron−barium−boron′ bond angle in **7** is 165.1(1)°, whereas **5** and **6** have linear boron−metal−boron′ angles. The smaller ionic radii of the metal ions in **5** and **6** probably force linear boron−metal−boron′ angles because of interligand steric interactions, while the larger ionic radius of the barium ion in **7** allows some bending.

Conclusions

Calcium, strontium, and barium complexes containing various tris(pyrazolyl)borate ligands have been synthesized and structurally characterized, and their volatilities and thermal stabilities were assessed. Complex **2** was structurally characterized, and exists with an unusual dimeric solid state structure. The remaining complexes adopt monomeric solid state structures with distorted octahedral geometries. The low thermal stability and volatility of **2** is likely related to its dimeric structure. Complexes **1** and **3**−**10** exhibit high thermal stabilities and volatilities, as demonstrated by the TGA traces, preparative sublimations, and melting point/decomposition determinations. Furthermore, **6**−**10** sublime as liquids, and are thus promising candidates for CVD and ALD film growth precursors. ALD growth studies employing the complexes described herein will be reported separately from our laboratory.

Experimental Section

General Considerations. All reactions were performed under argon using standard glovebox or Schlenk line techniques. THF was distilled from sodium benzophenone ketyl. Hexane was distilled from P_2O_5. KTp,[24] KTp^{Me2},[33] MTp_2 (M = Sr, **1**; Ba, **2**),[24] MTp_2^{Me2} (M = Sr, **3**; Ba, **4**),[25d] 3,5-diethylpyrazole,[34] 3,5-di-*n*-propylpyrazole,[34] and the *β*-diketones[35] used for the pyrazole syntheses were prepared according to literature procedures. $BaI_2(THF)_3$ was prepared by treating a slight excess of barium (1.1 equiv) with iodine (1.0 equiv) in refluxing THF. The number of THF ligands was estimated by the weight loss observed in the TGA trace. All other chemicals and solvents were purchased from Acros.

^1H and $^{13}C\{^1H\}$ NMR spectra were obtained at 400, 300, 125, or 75 MHz in dichloromethane-d_2 or benzene-d_6, as indicated. Infrared spectra were obtained using Nujol as the medium. Elemental analyses were performed by Midwest Microlab, Indianapolis, IN. It was necessary to add V_2O_5 as a combustion enhancing agent for **10** to obtain acceptable carbon values. Melting points were obtained on a Haake-Buchler HBI digital melting point apparatus or an Electrothermal Model 9200 melting point apparatus and are uncorrected. TGA was conducted on a Perkin-Elmer Pyris 1 TGA system between 25 and 450 °C, using nitrogen as the flow gas with a heating rate of 10 °C/min.

$SrTp_2$ (1). The analytical sample was obtained by sublimation at 200 °C/0.05 Torr: mp 273−275 °C; IR (Nujol, cm^{-1}) ν_{B-H} = 2529, ν_{C-N} = 1533; ^1H NMR (CD_2Cl_2, 23 °C, δ) 7.82 (d, J = 1.8 Hz, 6H, C*H*), 7.62 (d, J = 1.8 Hz, 6H, C*H*), 6.24 (t, J = 2.0 Hz, 6H, 4-C*H*), 4.8 (broad s, 2H, B−H); $^{13}C\{^1H\}$ NMR (CD_2Cl_2, 23 °C, ppm) 140.97 (s, *C*-H), 136.76 (s, *C*-H), 104.45 (s, 4-*C*H).

Anal. Calcd for $C_{18}H_{20}B_2N_{12}Sr$: C, 42.09; H, 3.92; N, 32.72. Found: C, 42.24; H, 4.01; N, 32.78.

$[BaTp_2]_2$ (2). The analytical sample was obtained by sublimation at 220 °C/0.05 Torr: mp 250−252 °C; IR (Nujol, cm^{-1}) ν_{B-H} = 2529, ν_{C-N} = 1533; ^1H NMR (toluene-d_8, 23 °C, δ) 7.57 (d, J = 1.8 Hz, 12H, C*H*), 7.03 (d, J = 1.8 Hz, 12H, C*H*), 5.97 (t, J = 1.8 Hz, 12H, 4-C*H*), 5.0 (broad s, 4H, B−H); ^1H NMR (toluene-d_8, −80 °C, δ) 7.76 (s, C*H*), 7.40 (s, C*H*), 7.29 (s, C*H*), 6.61 (s, C*H*), 6.07 (s, C*H*), 5.81 (s, C*H*); $^{13}C\{^1H\}$ NMR (CD_2Cl_2, 23 °C, ppm) 140.60 (s, *C*-H), 136.63 (s, *C*-H), 104.55 (s, 4-*C*H).

---

(30) Williams, R. A.; Hanusa, T. P.; Huffman, J. C. *Organometallics* **1990**, *9*, 1128–1134.

(31) Williams, R. A.; Tesh, R. F.; Hanusa, T. P. *J. Am. Chem. Soc.* **1991**, *113*, 4843–4851.

(32) Harvey, M. J.; Quisenberry, K. T.; Hanusa, T. P.; Young, V. G.Jr. *Eur. J. Inorg. Chem.* **2003**, 3383–3390.

(33) Trofimenko, S. *J. Am. Chem. Soc.* **1967**, *89*, 6288–6294.

(34) Noyce, D. S.; Ryder, E.Jr.; Walker, B. H. *J. Am. Chem. Soc.* **1955**, *20*, 1681–1686.

(35) Swamer, F. W.; Hauser, C. R. *J. Am. Chem. Soc.* **1950**, *72*, 1352–1356.

Anal. Calcd for $C_{36}H_{40}B_4Ba_2N_{24}$: C, 38.37; H, 3.58; N, 29.83. Found: C, 38.25; H, 3.38; N, 29.68.

Preparation of KTp$^{\mathrm{Et2}}$. A 50 mL round-bottomed flask was charged with potassium borohydride (1.711 g, 0.0317mol), 3,5-diethylpyrazole (13.400 g, 0.108 mol), and a stir bar. The mixture was slowly heated in an oil bath to 190 °C, while carefully monitoring hydrogen evolution. Once the gas evolution ceased (~2.3 L of H_2 collected), the hot oil bath was removed, and the reaction mixture was cooled to ~140 °C, at which point hexane (15 mL) was added. The reaction mixture was placed in a freezer at −23 °C for 2 h, resulting in the formation of a white precipitate. The white solid was collected by vacuum filtration on a medium glass frit and was washed with cold hexane (40 mL) to afford KTp$^{\mathrm{Et2}}$ as a white powder (8.102 g, 61%): mp 189−191 °C; IR (Nujol, cm^{-1}) $\nu_{\mathrm{B-H}}$ = 2444, $\nu_{\mathrm{C-N}}$ = 1534; ^{1}H NMR ($\mathrm{CD_2Cl_2}$, 23 °C, δ) 5.82 (s, 3H, 4-C*H*), 4.7 (broad s, 1H, B−H), 2.65 (q, *J* = 7.6 Hz, 6H, $\mathrm{CH_3C}\mathit{H}_2$), 2.54 (q, *J* = 7.5 Hz, 6H, $\mathrm{CH_3C}\mathit{H}_2$), 1.20 (t, *J* = 7.4 Hz, 9H, $\mathrm{C}\mathit{H}_3\mathrm{CH_2}$), 1.08 (t, *J* = 7.6 Hz, 9H, $\mathrm{C}\mathit{H}_3\mathrm{CH_2}$); ^{13}C{^{1}H} NMR ($\mathrm{CD_2Cl_2}$, 23 °C, ppm) 153.70 (s, C_{q}), 151.23 (s, C_{q}), 100.48 (s, 4-*C*H), 22.20 (s, $\mathrm{CH_3}\mathit{C}\mathrm{H_2}$), 20.67 (s, $\mathrm{CH_3}\mathit{C}\mathrm{H_2}$), 14.30 (s, $\mathit{C}\mathrm{H_3CH_2}$) 13.71 (s, $\mathit{C}\mathrm{H_3CH_2}$).

Anal. Calcd for $C_{21}H_{34}BKN_6$: C, 59.99; H, 8.15; N, 19.99. Found: C, 60.36; H, 8.13; N, 20.26.

Preparation of KTp$^{\mathrm{nPr2}}$. In a similar fashion to the preparation of KTp$^{\mathrm{Et2}}$, treatment of potassium borohydride (2.117 g, 0.0392 mol) with 3,5-di-*n*-propylpyrazole (20.000 g, 0.131 mol) afforded KTp$^{\mathrm{nPr2}}$ as a white powder (6.148 g, 31%): mp 109−110 °C; IR (Nujol, cm^{-1}) $\nu_{\mathrm{B-H}}$ = 2444, $\nu_{\mathrm{C-N}}$ = 1533; ^{1}H NMR ($\mathrm{CD_2Cl_2}$, 23 °C, δ) 5.77 (s, 3H, 4-C*H*), 4.7 (broad s, 1H, B−H), 2.58 (t, *J* = 7.5 Hz, 6H, $\mathrm{C}\mathit{H}_2\mathrm{CH_2CH_3}$), 2.46 (t, *J* = 7.8 Hz, 6H, $\mathrm{C}\mathit{H}_2\mathrm{CH_2CH_3}$), 1.59 (sextet, *J* = 7.7 Hz, 6H, $\mathrm{CH_2C}\mathit{H}_2\mathrm{CH_3}$), 1.44 (sextet, *J* = 7.5 Hz, 6H, $\mathrm{CH_2C}\mathit{H}_2\mathrm{CH_3}$) 0.95 (t, *J* = 7.4 Hz, 9H, $\mathrm{CH_2CH_2C}\mathit{H}_3$), 0.89 (t, *J* = 7.4 Hz, 9H, $\mathrm{CH_2CH_2C}\mathit{H}_3$); ^{13}C{^{1}H} NMR ($\mathrm{CD_2Cl_2}$, 23 °C, ppm) 152.13 (s, C_{q}), 149.63 (s, C_{q}), 101.70 (s, 4-*C*H), 31.35 (s, $\mathit{C}\mathrm{H_2CH_2CH_3}$), 29.56 (s, $\mathit{C}\mathrm{H_2CH_2CH_3}$), 23.62 (s, $\mathrm{CH_2}\mathit{C}\mathrm{H_2CH_3}$), 22.91 (s, $\mathrm{CH_2}\mathit{C}\mathrm{H_2CH_3}$), 14.41 (s, $\mathrm{CH_2CH_2}\mathit{C}\mathrm{H_3}$), 14.30 (s, $\mathrm{CH_2CH_2}\mathit{C}\mathrm{H_3}$).

Anal. Calcd for $C_{27}H_{46}BKN_6$: C, 64.27; H, 9.19; N, 16.65. Found: C, 64.46; H, 9.02; N, 16.73.

Preparation of CaTp$_2^{\mathrm{Et2}}$ (5). A 250 mL Schlenk flask was charged with $\mathrm{CaI_2}$ (0.372 g, 1.27 mmol), KTp$^{\mathrm{Et2}}$ (1.047 g, 2.49 mmol), and a stir bar. THF (100 mL) was added, resulting in the immediate formation of a white precipitate. The reaction mixture was stirred for 18 h, at which time the volatile components were removed under reduced pressure to afford a white residue. Hexane (50 mL) was added to the residue, and the resulting mixture was filtered through a 3 cm pad of Celite on a medium glass frit to yield a clear filtrate. Removal of the volatile components under reduced pressure afforded **5** as a white powder (0.804 g, 64%). The analytical sample and single crystals for the X-ray crystallographic analysis were obtained by crystallization from hexane at −23 °C: mp 225−226 °C; IR (Nujol, cm^{-1}) $\nu_{\mathrm{B-H}}$ = 2529, $\nu_{\mathrm{C-N}}$ = 1533; ^{1}H NMR ($\mathrm{CD_2Cl_2}$, 23 °C, δ) 5.80 (s, 6H, 4-C*H*), 4.8 (broad s, 2H, B−H), 2.90 (q, *J* = 7.5 Hz, 12H, $\mathrm{C}\mathit{H}_2\mathrm{CH_3}$), 2.08 (q, *J* = 7.5 Hz, 12H, $\mathrm{C}\mathit{H}_2\mathrm{CH_3}$), 1.25 (t, *J* = 7.7 Hz, 18H, $\mathrm{CH_2C}\mathit{H}_3$), 0.95 (t, *J* = 7.7 Hz, 18H, $\mathrm{CH_2C}\mathit{H}_3$); ^{13}C {^{1}H} NMR ($\mathrm{CD_2Cl_2}$, 23 °C, ppm) 155.35 (s, C_{q}), 151.44 (s, C_{q}), 100.43 (s, 4-*C*H), 21.14 (s, $\mathit{C}\mathrm{H_2CH_3}$), 20.78 (s, $\mathit{C}\mathrm{H_2CH_3}$), 13.57 (s, $\mathrm{CH_2}\mathit{C}\mathrm{H_3}$), 13.30 (s, $\mathrm{CH_2}\mathit{C}\mathrm{H_3}$).

Anal. Calcd for $C_{42}H_{68}B_2CaN_{12}$: C, 62.83; H, 8.54; N, 20.94. Found: C, 62.89; H, 8.45; N, 21.01.

Preparation of SrTp$_2^{\mathrm{Et2}}$ (6). In a fashion similar to the preparation of **5**, treatment of $\mathrm{SrI_2}$ (0.817 g, 2.39 mmol) with KTp$^{\mathrm{Et2}}$ (1.978 g, 4.70 mmol) afforded **6** as a white solid (1.274 g, 64%). The analytical sample and single crystals for the X-ray crystallographic analysis were obtained by crystallization from hexane at −23 °C: mp 188−190 °C; IR (Nujol, cm^{-1}) $\nu_{\mathrm{B-H}}$ = 2532, $\nu_{\mathrm{C-N}}$ = 1533; ^{1}H NMR ($\mathrm{CD_2Cl_2}$, 23 °C, δ) 5.82 (s, 6H, 4-C*H*), 4.8 (broad s, 2H, B−H), 2.87 (q, *J* = 7.5 Hz, 12H, $\mathrm{C}\mathit{H}_2\mathrm{CH_3}$), 2.22 (q, *J* = 7.5 Hz, 12H, $\mathrm{C}\mathit{H}_2\mathrm{CH_3}$), 1.25 (t, *J* = 7.4 Hz, 18H, $\mathrm{CH_2C}\mathit{H}_3$), 1.01 (t, *J* = 7.7 Hz, 18H, $\mathrm{CH_2C}\mathit{H}_3$); ^{13}C {^{1}H} NMR ($\mathrm{CD_2Cl_2}$, 23 °C, ppm) 154.96 (s, C_{q}), 151.81 (s, C_{q}), 100.58 (s, 4-*C*H), 21.38 (s, $\mathit{C}\mathrm{H_2CH_3}$), 21.18 (s, $\mathit{C}\mathrm{H_2CH_3}$), 13.69 (s, $\mathrm{CH_2}\mathit{C}\mathrm{H_3}$), 13.57 (s, $\mathrm{CH_2}\mathit{C}\mathrm{H_3}$).

Anal. Calcd for $C_{42}H_{68}B_2N_{12}Sr$: C, 59.32; H, 8.06; N, 19.77. Found: C, 59.04; H, 7.79; N, 19.82.

Preparation of BaTp$_2^{\mathrm{Et2}}$ (7). A 250 mL Schlenk flask was charged with $\mathrm{BaI_2(THF)_3}$ (0.689 g, 1.134 mmol), KTp$^{\mathrm{Et2}}$ (0.934 g, 2.221 mmol), and a stir bar. THF (80 mL) was added, resulting in the immediate formation of a white precipitate. The reaction mixture was stirred for 18 h, at which point the volatile components were removed under reduced pressure to afford a white residue. Hexane (60 mL) was added, and the resulting mixture was filtered through a 3 cm pad of Celite on a medium glass frit to yield a clear, colorless filtrate. The filtrate was reduced in volume under reduced pressure to about 20 mL, and the flask was placed in the freezer at −23 °C for 18 h. Removal of the solvent by cannula, followed by vacuum drying, afforded colorless crystals of **7** (0.686 g, 67%): mp 129−131 °C; IR (Nujol, cm^{-1}) $\nu_{\mathrm{B-H}}$ = 2526, $\nu_{\mathrm{C-N}}$ = 1532; ^{1}H NMR ($\mathrm{CD_2Cl_2}$, 23 °C, δ) 5.82 (s, 6H, 4-C*H*), 4.8 (broad s, 2H, B−H), 2.79 (q, *J* = 7.3 Hz, 12H, $\mathrm{C}\mathit{H}_2\mathrm{CH_3}$), 2.28 (q, *J* = 7.5 Hz, 12H, $\mathrm{C}\mathit{H}_2\mathrm{CH_3}$), 1.17 (t, *J* = 7.4 Hz, 18H, $\mathrm{CH_2C}\mathit{H}_3$), 1.04 (t, *J* = 7.8 Hz, 18H, $\mathrm{CH_2C}\mathit{H}_3$); ^{13}C{^{1}H} NMR ($\mathrm{CD_2Cl_2}$, 23 °C, ppm) 154.31 (s, C_{q}), 151.68 (s, C_{q}), 100.85 (s, 4-*C*H), 21.49 (s, $\mathit{C}\mathrm{H_2CH_3}$), 21.00 (s, $\mathit{C}\mathrm{H_2CH_3}$), 13.99 (s, $\mathrm{CH_2}\mathit{C}\mathrm{H_3}$), 13.64 (s, $\mathrm{CH_2}\mathit{C}\mathrm{H_3}$).

Anal. Calcd for $C_{42}H_{68}B_2N_{12}Ba$: C, 56.04; H, 7.62; N, 18.80. Found: C, 55.96; H, 7.76; N, 18.80.

Preparation of CaTp$_2^{\mathrm{nPr2}}$ (8). In a fashion similar to the preparation of **5**, treatment of $\mathrm{CaI_2}$ (0.150 g, 0.510 mmol) with KTp$^{\mathrm{nPr2}}$ (0.515 g, 1.02 mmol) afforded **8** as a white solid (0.250 g, 51%). The analytical sample and single crystals for the X-ray crystallographic analysis were obtained by crystallization from hexane at −23 °C: mp 169−172 °C; IR (Nujol, cm^{-1}) $\nu_{\mathrm{B-H}}$ = 2517, $\nu_{\mathrm{C-N}}$ = 1532; ^{1}H NMR ($\mathrm{CD_2Cl_2}$, 23 °C, δ) 5.76 (s, 6H, 4-C*H*), 4.8 (broad s, 2H, B−H), 2.82 (t, *J* = 7.5 Hz, 12H, $\mathrm{C}\mathit{H}_2\mathrm{CH_2CH_3}$), 1.59 (t, *J* = 8.1 Hz, 12H, $\mathrm{C}\mathit{H}_2\mathrm{CH_2CH_3}$), 1.59 (sextet, *J* = 7.4 Hz, 12H, $\mathrm{CH_2C}\mathit{H}_2\mathrm{CH_3}$), 1.38 (sextet, *J* = 7.7 Hz, 12H, $\mathrm{CH_2C}\mathit{H}_2\mathrm{CH_3}$), 0.96 (t, *J* = 7.4 Hz, 18H, $\mathrm{CH_2CH_2C}\mathit{H}_3$), 0.66 (t, *J* = 7.4 Hz, 18H, $\mathrm{CH_2CH_2C}\mathit{H}_3$); ^{13}C {^{1}H} NMR ($\mathrm{CD_2Cl_2}$, 23 °C, ppm) 154.08 (s, C_{q}), 149.79 (s, C_{q}), 101.68 (s, 4-*C*H), 29.89 (s, $\mathit{C}\mathrm{H_2CH_2CH_3}$), 29.76 (s, $\mathit{C}\mathrm{H_2CH_2CH_3}$), 23.20 (s, $\mathrm{CH_2}\mathit{C}\mathrm{H_2CH_3}$), 22.59 (s, $\mathrm{CH_2}\mathit{C}\mathrm{H_2CH_3}$), 14.35 (s, $\mathrm{CH_2CH_2}\mathit{C}\mathrm{H_3}$), 14.18 (s, $\mathrm{CH_2CH_2}\mathit{C}\mathrm{H_3}$).

Anal. Calcd for $C_{54}H_{92}B_2CaN_{12}$: C, 66.78; H, 9.55; N, 17.31. Found: C, 67.02; H, 9.27; N, 17.56.

Preparation of SrTp$_2^{\mathrm{nPr2}}$ (9). In a fashion similar to the preparation of **5**, treatment of $\mathrm{SrI_2}$ (0.340 g, 0.996 mmol) with KTp$^{\mathrm{nPr2}}$ (0.991 g, 1.96 mmol) afforded **9** as a white solid (0.750 g, 75%). The analytical sample and single crystals for the X-ray crystallographic analysis were obtained by crystallization from hexane at −23 °C: mp 164−168 °C; IR (Nujol, cm^{-1}) $\nu_{\mathrm{B-H}}$ = 2511, $\nu_{\mathrm{C-N}}$ = 1532; ^{1}H NMR ($\mathrm{CD_2Cl_2}$, 23 °C, δ) 5.76 (s, 6H, 4-C*H*), 4.8 (broad s, 2H, B−H), 2.78 (t, *J* = 7.7 Hz, 12H, $\mathrm{C}\mathit{H}_2\mathrm{CH_2CH_3}$), 2.11 (t, *J* = 8.1 Hz, 12H, $\mathrm{C}\mathit{H}_2\mathrm{CH_2CH_3}$), 1.57 (sextet, *J* = 7.5 Hz, 12H, $\mathrm{CH_2C}\mathit{H}_2\mathrm{CH_3}$), 1.41 (sextet, *J* = 7.9 Hz, 12H, $\mathrm{CH_2C}\mathit{H}_2\mathrm{CH_3}$), 0.95 (t, *J* = 7.4 Hz, 18H, $\mathrm{CH_2CH_2C}\mathit{H}_3$), 0.70 (t, *J* = 7.7 Hz, 18H, $\mathrm{CH_2CH_2C}\mathit{H}_3$); ^{13}C {^{1}H} NMR ($\mathrm{CD_2Cl_2}$, 23 °C, ppm) 153.56 (s, C_{q}), 150.07 (s, C_{q}), 101.88 (s, 4-*C*H), 30.43 (s, $\mathit{C}\mathrm{H_2CH_2CH_3}$), 29.80 (s, $\mathit{C}\mathrm{H_2CH_2CH_3}$), 23.02 (s, $\mathrm{CH_2}\mathit{C}\mathrm{H_2CH_3}$), 22.96 (s, $\mathrm{CH_2}\mathit{C}\mathrm{H_2CH_3}$), 14.26 (s, $\mathrm{CH_2CH_2}\mathit{C}\mathrm{H_3}$), 14.21 (s, $\mathrm{CH_2CH_2}\mathit{C}\mathrm{H_3}$).

Anal. Calcd for $C_{54}H_{92}B_2N_{12}Sr$: C, 63.67; H, 9.10; N, 16.57. Found: C, 63.48; H, 8.97; N, 16.57.

Preparation of BaTp$_2^{\mathrm{nPr2}}$ (10). In a fashion similar to the preparation of **5**, treatment of $\mathrm{BaI_2(THF)_3}$ (1.65 g, 2.74 mmol) with KTp^{nPr2} (1.00 g, 5.49 mmol) afforded **10** as a colorless, waxy solid (0.54 g, 39%). The analytical sample was obtained by sublimation at 240 °C/0.05 Torr: mp 141−144 °C; IR (Nujol, cm^{-1}) $\nu_{B-H} = 2470$, $\nu_{C-N} = 1532$; ^1H NMR (CD_2Cl_2, 23 °C, δ) 5.77 (s, 6H, 4-C*H*), 4.8 (broad s, 2H, B−H), 2.71 (t, $J = 7.6$ Hz, 12H, $CH_2CH_2CH_3$), 2.21 (t, $J = 8.2$ Hz, 12H, $CH_2CH_2CH_3$), 1.51 (sextet, $J = 7.6$ Hz, 12H, $CH_2CH_2CH_3$), 1.46 (sextet, $J = 7.5$ Hz, 12H, $CH_2CH_2CH_3$), 0.93 (t, $J = 7.2$ Hz, 18H, $CH_2CH_2CH_3$), 0.74 (t, $J = 7.4$ Hz, 18H, $CH_2CH_2CH_3$); $^{13}C\{^1H\}$ NMR (C_6D_6, 23 °C, ppm) 152.47 (s, C_q), 149.96 (s, C_q), 102.78 (s, 4-*C*H), 30.82 (s, $CH_2CH_2CH_3$), 29.59 (s, $CH_2CH_2CH_3$), 23.65 (s, $CH_2CH_2CH_3$), 22.80 (s, $CH_2CH_2CH_3$), 14.32 (s, $CH_2CH_2CH_3$), 14.07 (s, $CH_2CH_2CH_3$).

Anal. Calcd for $C_{54}H_{92}B_2BaN_{12}$: C, 60.70; H, 8.68; N, 15.74. Found: C, 60.97; H, 8.77; N, 15.79.

Preparative Sublimation Studies. For the sublimation experiments, 2.5 cm diameter, 30 cm long glass tubes were employed. One end of the tube was sealed, and the other end was equipped with a 24/40 male glass joint. In an argon-filled glovebox, the compound to be sublimed (0.5−1.0 g) was loaded into a 1.0 × 4.0 cm glass tube, and this tube was placed at the sealed end of the glass sublimation tube. The sublimation tube was fitted with a 24/40 vacuum adapter, and then was inserted into a horizontal Buchi Kugelrohr oven such that about 15 cm of the tube was situated in the oven. A vacuum of 0.05 Torr was established, and the oven was heated to the indicated temperature. The compounds sublimed to the cool zone just outside of the oven. The percent recovery was obtained by weighing the sublimed product. The percent nonvolatile residue was calculated by weighing the 1.0 × 4.0 cm glass tube at the end of the sublimation. Data are given in the text and in Table 7.

Thermal Decomposition Studies. In an argon-filled drybox, a melting point capillary tube was charged with 1−2 mg of a sample of **1**−**10**, and the end of the tube was sealed with a small amount of stopcock grease. The capillary tube was then removed from the drybox, and the end was flame-sealed. The capillary tube was transferred to an Electrothermal Model 9200 melting point apparatus and was then heated at 5 °C/min from 25 to 400 °C. In this fashion, samples of **1**−**10** were visually observed for discoloration or other evidence of decomposition over the 75 min experiments. This procedure allowed qualitative assessment of thermal stability up to 400 °C. Data are given in the text and in Table 7.

X-ray Crystallographic Structure Determinations for 1, 2, and 5−7. Diffraction data were measured on a Bruker X8 APEX-II kappa geometry diffractometer with Mo radiation and a graphite monochromator. Frames were collected at 100 K with the detector at 40 mm, 0.3° between each frame, and were recorded for 5−10 s. APEX-II[36] and SHELX[37] software were used in the collection and refinement of the models. Crystals of **1** grew as colorless rods upon sublimation. These crystals were all twinned; more than 6 specimens were assayed. A twinned sample was selected, and the structure was satisfactorily extracted using software Cell_Now and TwinAbs, which found a 180° twin rotation about the 13 Å axis. 62310 reflections were measured, yielding 6845 unique data. Hydrogen atoms were placed in calculated and observed positions. The asymmetric unit contains two half-molecules with Sr(1) and Sr(2) each occupying a crystallographic inversion center. Crystals of **2** were colorless and irregular. 87104 reflections were counted, which averaged to 9769 independent data. Hydrogen atoms were placed at calculated or observed positions. All atoms occupy general positions in the cell, but the molecule itself occupies a crystallographic inversion center. Disorder was observed for one portion of the ligand, consequently B(1), N(5), N(6), C(7), C(8), and C(9) were assigned 50/50 partial positions and kept isotropic. Complex **5** crystallized as colorless parallelepipeds. 65160 *hkl* data points were harvested, which averaged to 5821 data. Hydrogen atoms were calculated, except that the H atom on B(1) was observed. The asymmetric unit contains one-half molecule with the Ca ion occupying a crystallographic inversion center. The two atoms C(19) and C(20) were assigned two half-positions each. Crystals of **6** were colorless rhomboids. 65719 reflections were counted, which averaged to 7210 independent data. Hydrogen atoms were calculated, except that the H atom on B(1) was observed. The asymmetric unit contains one-half molecule, with the Sr ion occupying a crystallographic inversion center. Crystals of **7** were colorless rods. 146747 data were integrated, which averaged into 12342 independent data. Hydrogen atoms were placed in observed or calculated positions. Two partial sites were assigned for the terminal atom C(33). All atoms occupy general positions in the cell.

Acknowledgment. We thank the Army Research Office (Grant W911NF-07-0489) for generous support of this research.

Supporting Information Available: X-ray crystallographic files in CIF format for the structure determinations of **1**, **2**, and **5**−**7**. This material is available free of charge via the Internet at http://pubs.acs.org.

---

[36] *APEX II, collection and processing programs*; Bruker AXS Inc.: Madison, WI, 2005

[37] Sheldrick, G. M. *Acta Crystallogr.* **2008**, *A64*, 112–122.